Journal of Basic and Applied Engineering Research
p-ISSN: 2350-0077; e-ISSN: 2350-0255; Volume 6, Issue 2; January-March, 2019, pp. 89-100

http://www.krishisanskriti.org/Publication.html

VELOCITY VARIATION IN MHD DOUBLE DIFFUSIVE CHEMICALLY REACTIING OF A MICROPOLAR FLUID FLOW IN A POROUS MEDIUM

V. Dabral[1], Ashok Kumar[2] and S. Kapoor[3]

[1]Department of Mathematics, HNB, Garhwal University, Srinagar
[2]Department of Mathematics, HNB, Garhwal University, Srinagar
[3]DESM, RIE(NCERT) Bhubaneswar
E-mail: [1]vandana.p96@gmail.com, [2]ashrsdma@gmail.com, [3]saurabh09.iitr@gmail.com

Abstract—*This present paper reports the study of the free convection, double diffusive incompressible micropolar fluid flow between two vertical parallel plates containing a Darcy-Forchheimer porous medium. Asymmetric wall temperatures and concentrations are present and take into account a temperature-dependent variable thermal conductivity. The similarity transformation approach is adopted to transformed system of non linear PDE equations to ODE which is named as linear momentum, angular momentum, energy and species. Computational simulation using the finite element method is done for the system of coupled differential equations. The effects of Darcy number (Da), Forchheimer number (Fs), Grashof number (Gr) and thermal conductivity parameter (S) on the velocity, angular velocity and temperature / concentration profiles are studied in detail. A comparison with another method has also been presented to show the compatibility of the proposed method..*

1. INTRODUCTION

Free convection in fluid saturated porous media constitutes an area of major activity in transport phenomena research owing to its application in a diverse number of fields including geothermal energy systems, enhanced recovery in petroleum reservoirs, filtration sciences, heat exchange between soil and atmosphere, transport of moisture through porous industrial materials and ceramic processing. The fundamental importance of convective flow in porous media has been well-reviewed in the recent book by Ingham and Pop(2002),Nield and Bejan (1999) have also addressed in detail the natural convective flows due to combined buoyant mechanisms in porous media. Rawat (2012) focused to develop a mathematical model for the comparative study of combined effects of free convective heat and mass transfer on the steady two-dimensional, laminar fluid flow past a moving permeable vertical surface subjected to a transverse uniform magnetic field. Rawat (2016) investigates the two dimensional flow, heat and mass transfer of chemically reacting Micropolarfluid over a non-linear stretching sheet with variable heat flux in a non-darcy porous mediumRawat&Kaoor (2017) studied Study of buoyancy driven free convective flow of a micropolar fluid through adarcy-forchheimer porous medium with mutable thermal conductivity.

The objective of the present investigation is to study numerically the natural convection heat and mass transfer of a fully developed micropolar fluid flow in a Darcy-Forchheimer porous medium for asymmetric wall temperatures and concentrations with temperature-dependent thermal conductivity. The governing partial differential equations for the flow are transformed and solved using finite element method. The model finds applications in polymer technology, aerodynamic heating, geophysics and ceramic processing..

2. MATHEMATICAL MODEL

Consider the laminar natural convection flow between two vertical plates in a homogenous, incompressible, micro polar fluid-saturated porous medium with temperature dependent thermal conductivity. The vertical plates are separated by a distance *b* with reference to an x, y coordinate system, where the x-axis is directed along the vertical plates and the y-axis is transverse to this. It is assumed that the two walls are maintained at different temperatures and concentrations resulting in an *asymmetric* situation with respect to temperature and concentration respectively. The flow is also assumed steady and fully developed i.e. transverse

velocity is zero and therefore the flow depends only on the transverse coordinate, *y*. The geometry of the system is shown in figure 1, neglecting viscous heating and thermal dispersion effects, under the Boussinesq approximation, the one-dimensional conservation equations may be presented as follows

Linear Momentum Equation:

$$(\mu+\kappa)\frac{d^2u}{dy^2}+k\frac{dg}{dy}+\rho\beta_T g_a(T-T_0)+\rho\beta_C g_a(C-C_0)-\sigma B_0^2 u-\frac{(\mu+\kappa)}{k_p}u-\frac{b_F\rho}{k_p}u^2=0$$

Angular Momentum Equation:

$$\gamma\frac{d^2g}{dy^2}-k\left(2g+\frac{du}{dy}\right)=0$$

4.3.3. Energy Equation:

$$\frac{d}{dy}\left(k_f\frac{dT}{dy}\right)+Q_0(T-T_0)=0$$

4.3.4. Diffusion Equation:

$$\frac{d^2C}{dy^2}-\Gamma(\boldsymbol{C}-\boldsymbol{C_0})=0$$

The corresponding boundary conditions on the vertical surfaces are:

$$y=0:u=0,g=0,T=T_1,C=C_1$$

$$y=b:u=0,g=0,T=T_2,C=C_2$$

Where μ , κ, k_p and b_F designate respectively the Newtonian dynamic viscosity, Eringen vortex viscosity, permeability and inertia coefficient of the porous medium respectively, $\gamma=\left(\mu+\frac{\kappa}{2}\right)j$, is the spin gradient viscosity i.e. gyro-viscosity, j denotes the microinertia density, u is the micropolar linear velocity, g is the angular velocity (micro-rotation) of the micropolar fluid micro-elements, k_f is the thermal conductivity of the fluid, T and C are the fluid temperature and concentration respectively, T_0 is the inlet temperature and C_0 is the inlet concentration. The left plate (i.e at y = 0) is kept at constant temperature T_1 and the right plate (i.e., at y = b) is maintained at a constant temperature T_2. Additionally, the concentration varies from C_1 on the left plate to C_2 on the right plate.

We also note that the micro-rotation conditions imposed at both plates correspond to the case where particle rotation (spin) at the wall is not permitted i.e. micro-element rotation vanishes. Such a scenario corresponds physically to concentrated particle flows. We further assume that the thermal conductivity is a function of temperature and is defined as:

$k_f=k_1[1+\propto(T-T_0)]$ or $k_f=k_1[1+S\theta]$ where $S=\alpha(T_1-T_0)$ (4.7)

Wherek_1 is the fluid thermal conductivity at temperature T_1 and α is a constant depending on the nature of the fluid. In general S>0 for water and air whereas, S<0 for fluids such as lubricating oils. Proceeding with the analysis, we introducing the similarity transformations:

$u=\frac{\mu Gr}{b\rho}U, y=Yb, g=\frac{\mu Gr}{b^2\rho}H, \theta=\frac{T-T_0}{T_1-T_0}, \Phi=\frac{C-C_0}{C_1-C_0}$(4.8)

Substitution into equations leads to the following set of non-linear, coupled, ordinary differential equations:

Linear Momentum Equation:

$$(1+R)\frac{d^2U}{dY^2}+R\frac{dH}{dY}+\theta+N_b\Phi-MU-\frac{(1+R)}{Da}U-\frac{FsGr}{Da}U^2=0 \quad (1)$$

Angular Momentum Equation:

$$\left(1+\frac{R}{2}\right)\frac{d^2H}{dY^2}-BR\left(2H+\frac{dU}{dY}\right)=0 \quad (2)$$

Energy Equation:

$$(1+\mathrm{S}\theta)\frac{\mathrm{d}^2\theta}{\mathrm{dY}^2}+\mathrm{S}\left(\frac{\mathrm{d}\theta}{\mathrm{dY}}\right)^2+h_s\theta=0 \qquad (3)$$

Diffusion Equation:

$$\left(\frac{d^2\Phi}{dY^2}\right)-\chi\Phi=0 \qquad (4)$$

Where$B=\frac{b^2}{j}$and $R=\frac{\kappa}{\mu}$are micropolar parameters (dimensionless material properties) and$N_b=\frac{\beta_C(C_1-C_0)}{\beta_T(T_1-T_0)}$is the buoyancy ratio,$Gr=\frac{g_a\beta_T b^3\rho^2}{\mu^2}(T_1-T_0)$ is the Grashof number, $Da=\frac{K_p}{b^2}$ is the Darcy number and$Fs=\frac{b_F}{b}$ is the Forchheimer (quadratic porous drag) number&$\chi=\frac{\mu\Gamma}{\mathrm{U}^2}$Is the chemically reacting parameter. The transformed boundary conditions now become:

At $Y=0:U=0,H=0,\theta=0,\Phi=1$ (5)

At $Y=1:U=0,H=0,\theta=m,\Phi=n$ (6)

Where$m=\frac{T_2-T_0}{T_1-T_0}$ is the wall temperature ratio and $\mathrm{n}=\frac{C_2-C_0}{C_1-C_0}$ is the wall concentration ratio. of special significance in engineering applications is the shear stress, the wall heat flux and wall heat transfer coefficient. The shear stress at the left wall is given by:

$$\tau_1=[(\mu+\kappa)\left(\frac{du}{dy}\right)+\kappa g]_{y=0}=\frac{(\mu+\kappa)Gr\mu}{\rho b^2}U'(0) \qquad (7S)$$

The heat flux at the left wall may be written using Fourier's law as follows:

$$q_1=-k_f\frac{dT}{dy}\Big|_{y=0}=-\frac{k_f(T_1-T_0)}{b}\theta'(0) \qquad (8)$$

The heat transfer coefficient at the left wall is given by:

$$h_1=\frac{q_1}{(T_1-T_0)}=-\frac{k_f}{b}\theta'(0) \qquad (9)$$

The Nusselt number at the left wall can be defined thus:

$$Nu=\frac{h_1 b}{k_f}=-\theta'(0) \qquad (10)$$

The dimensionless volume flow rate is given by:

$$Q=\int_0^1 UdY \qquad (11)$$

The dimensionless total heat rate added to the fluid is given by :$E=\int_0^1 U\theta dY$ (12)

Finally the dimensionless total species rate added to the fluid is given by:

$$\psi=\int_0^1 U\Phi dY \qquad (13)$$

Additionally the wall couple stress at both plates can be defined by:

$M_w=\left[\gamma\frac{\partial g}{\partial y}\right]at\ y=0$ (left plate) and $M_w=\left[\gamma\frac{\partial g}{\partial y}\right]at\ y=1$ (right plate) (14)

3. NUMERICAL SOLUTION USING FEM

The transformed two-point boundary value problem is solved numerically using FEM. The entire domain is split into a set of 81 line elements of having equal width, containing two node.

Vibrational formulation:

The vibrational formulation corresponding to the equations over a typical two noded linear element (Y_e, Y_{e+1}) is given by

$$\int_{Y_e}^{Y_{e+1}} w_1 \left\{(1+R)\frac{d^2U}{dY^2} + R\frac{dH}{dY} + \theta + N_b\Phi - \mathrm{MU} - \frac{(1+R)}{Da}U - \frac{FsGr}{Da}U^2\right\} dY = 0 \quad (15)$$

$$\int_{Y_e}^{Y_{e+1}} w_2 \left\{\left(1+\frac{R}{2}\right)\frac{d^2H}{dY^2} - BR(2H + \frac{dU}{dY})\right\} dY = 0 \ (16)$$

$$\int_{Y_e}^{Y_{e+1}} w_3 \left\{(1+S\theta)\frac{d^2\theta}{dY^2} + S\left(\frac{d\theta}{dY}\right)^2 + h_s\theta\right\} dY = 0 \qquad (17)$$

$$\int_{Y_e}^{Y_{e+1}} w_4 \left\{\frac{\partial^2\Phi}{\partial Y^2} - \chi\Phi\right\} dY = 0 \qquad (18)$$

Where$w_1, w_2, w_3\ and\ w_4$ are arbitrary test functions and may be viewed as the variation in $U, H, \theta\ and\ \Phi$ respectively.

Finite element formulation:

The finite element formulation might be obtained from equations by substituting finite element approximations:

$$U = \sum_{j=1}^{2} U_j\psi_j\,, H = \sum_{j=1}^{2} H_j\psi_j\,, \theta = \sum_{j=1}^{2} \theta_j\psi_j\ \,, \Phi = \sum_{j=1}^{2} \theta_j\psi_j \qquad (19)$$

With $w_1 = w_2 = w_3 = w_4 = \psi_i\ (i = 1{,}20)$ where ψ_i are the shape functions for a typical element (Y_e, Y_{e+1}) and are taken as: $\psi_1^{(e)} = \frac{Y_{e+1}-Y}{Y_{e+1}-Y_e}, \psi_2^{(e)} = \frac{Y\ -Y_e}{Y_{e+1}-Y_e}\,, for\ Y_e \le Y \le Y_{e+1} \qquad (20)$

The finite element model of the equations for a typical element (Y_e, Y_{e+1}) thus formed is given by: $U, H, \theta\ and\ \Phi$

$$\begin{bmatrix} [K^{11}][K^{12}][K^{13}][K^{14}] \\ [K^{21}][K^{22}][K^{23}][K^{24}] \\ [K^{31}][K^{32}][K^{33}][K^{34}] \\ [K^{41}][K^{42}][K^{43}][K^{44}] \\ [K^{51}]\ K^{52}\ \ K^{53}\ \ K^{54} \\ \qquad K^{mn} \end{bmatrix} \begin{bmatrix} \{U\} \\ \{H\} \\ \{\theta\} \\ \{\Phi\} \end{bmatrix} = \begin{bmatrix} \{b^1\} \\ \{b^2\} \\ \{b^3\} \\ \{b^4\} \end{bmatrix} (20)$$

Where$[K^{mn}]$and$[b^m]$ (m,n=1,2,3,4,) are the matrices of order $2x2\ and\ , 2x1$ respectively. All these matrices may be defined as follows:

$$K_{ij}^{11} = -(1+R)\int_{Y_e}^{Y_{e+1}} \frac{d\psi_i}{dY}\frac{d\psi_j}{dY}dY\ - M\int_{Y_e}^{Y_{e+1}} \psi_i\psi_j dY - \frac{(1+R)}{Da}\int_{Y_e}^{Y_{e+1}} \psi_i\psi_j dY$$
$$- \frac{FsGr}{Da}\overline{U_1}\int_{Y_e}^{Y_{e+1}} \psi_i\psi_1\psi_j dY - \frac{FsGr}{Da}\overline{U_2}\int_{Y_e}^{Y_{e+1}} \psi_i\psi_2\psi_j dY$$

$K_{ij}^{12} = R\int_{Y_e}^{Y_{e+1}} \psi_i\frac{d\psi_j}{dY}dY\ , K_{ij}^{14} = N_b\int_{Y_e}^{Y_{e+1}} \psi_i\psi_j dY$

$$K_{ij}^{21} = -BR\int_{Y_e}^{Y_{e+1}} \psi_i\frac{d\psi_j}{dY}dY$$

$$K_{ij}^{22} = -\left(1+\frac{R}{2}\right)\int_{Y_e}^{Y_{e+1}} \frac{d\psi_i}{dY}\frac{d\psi_j}{dY}dY - 2BR\int_{Y_e}^{Y_{e+1}} \psi_i\psi_j dY$$

$K_{ij}^{23} = K_{ij}^{24} = 0, K_{ij}^{31} = K_{ij}^{32} = 0$

$$K_{ij}^{33} = -\int_{Y_e}^{Y_{e+1}} \frac{d\psi_i}{dY}\frac{d\psi_j}{dY}dY\ - S\,\overline{\theta_1}\int_{Y_e}^{Y_{e+1}} \psi_1\frac{d\psi_i}{dY}\frac{d\psi_j}{dY}dY\ - S\overline{\theta_2}\int_{Y_e}^{Y_{e+1}} \psi_2\frac{d\psi_i}{dY}\frac{d\psi_j}{dY}dY$$

$K_{ij}^{34} = 0, K_{ij}^{41} = K_{ij}^{42} = K_{ij}^{43}\ = 0$

$$K_{ij}^{44} = -\int_{Y_e}^{Y_{e+1}} \frac{d\psi_i}{dY}\frac{d\psi_j}{dY}dY$$

$$b_i^1 = -\left(\psi_i \frac{d\mathrm{U}}{dY}\right)_{Y_e}^{Y_{e+1}}, \; b_i^2 = -\left(\psi_i \frac{d\mathrm{H}}{dY}\right)_{Y_e}^{Y_{e+1}}$$

$$b_i^3 = -\left(\psi_i \frac{d\theta}{dY}\right)_{Y_e}^{Y_{e+1}} - s\,\overline{\theta_1}\left(\psi_1\psi_i \frac{d\theta}{dY}\right)_{Y_e}^{Y_{e+1}} - s\,\overline{\theta_2}\left(\psi_2\psi_i \frac{d\theta}{dY}\right)_{Y_e}^{Y_{e+1}}$$

$$b_i^4 = -\left(\psi_i \frac{d\Phi}{dY}\right)_{Y_e}^{Y_{e+1}} \quad (21)$$

Where

$$\overline{U} = \sum_{i=1}^{2} \overline{U}_i\psi_i \;, \bar{\theta} = \sum_{i=1}^{2} \bar{\theta}_i\psi_i \quad (22)$$

Each element matrix is of the order$8x8$. Since the whole domain is divided into a set of 81 line elements. Thus after assembly of all the elements equations we obtain a matrix of order$328x328$. This system of equations as obtained is non-linear therefore an iterative scheme has been used to solve it. The system is linearized by incorporating the functions $\overline{U}$ and$\bar{\theta}$, which are assumed to be known. After applying the given boundary conditions, only a system of 320 equations remains for the solution which has been solved by the Gauss-Seidel method maintaining an accuracy of 0.0005.

4. RESULTS AND DISCUSSION

In order to verify the results the numerical computation verification is shown in Table 1 and 2,2 respectively. In Table 1 the skin friction and wall heat transfer rates at the left plate, $U'(0)$ and $-\theta'(0)$ in **is shown**. Here, we observe that increasing the thermal conductivity parameter, S, greatly increases the rate of heat transfer at the left wall. However the skin friction at the left wall is reduced with a rise in thermal conductivity parameter i.e. the micropolar fluid is decelerated at the left plate with a rise in S from 0 to 0.4. From, Table 2. we have seen that the method well accurate in respect to the another existing method . The present finite element solutions are highly accurate

In this section rigours study has been made for numerical experiment. The variation of distinguished physical parameters, like Darcy number (Da), Forchheimer drag (Fs), Grahof Number (Gr),micropolar parameters(R), Chemically reacting parameter (χ), Buoyancy ratio (N_b) on flow dynamics is shown in this section. Whereas some physical parameters $(N_b = 2, B = 1, m = 0.2, n = 0.1)$ were fixed at certain level throughout the study duringnumerical computations. The computed study will illustrate graphically.

Figures **2,** shows the effect of Darcy number (Da) on velocity (U) and angular velocity (H) with respect to the characteristics length (Y) during study of boundary layer flow. Here, this has been observed that the translational velocity (U) of micropolar fluid is increase for higher values of Darcy number (Da) as expected since Da is directly proportional to the permeability of the porous medium. Here the Darcy number (Da) is taken as $Da = 5x10^{-2}$, 5x10^{-1}, 10^{-1},1, 2 .This exerted that, high porosity porous medium exerts less resistance to flow. Hence the micropolar fluid is accelerated that is translational momentum is boosted, with the rise in Da. Figure 3, we observe that values of micro-rotation are negative in the first half whereas in the second half, these are positive, thus showing a reverse rotation near the two boundaries. Close examination of figure 3 reveals that micro-rotation, H, actually vanishes in the zone, 0.25 < H < 0.375, and this vanishing location drifts closer to the centre-line of the channel as Da values increase from 0.05 through 0.1, 0.5, 1 and 2. Micro-elements therefore do not perform rotary motions as the curves cross the Y axis. An increase in the Darcy number leads to an increase in micro-rotation. So the porosity of the medium can be used effectively to increase or decrease the angular rotation commonly arising in suspension flows in porous lubrication problems e.g. porous journal bearings . We note that for the limiting case of Da $\rightarrow\infty$, the fibers of the porous matrix vanish and the regime becomes purely fluid i.e. infinite permeability (hydraulic conductivity). Figures 4 to 5 show the effect of Forchheimer (inertial porous) parameter on the translational and angular velocity profiles. For the case of $Fs = 0$ the regime is Darcian. A rise in Da from 10 (weakly imposed quadratic drag) to 40, retards the flow development and decreases the velocity, U. In the Darcy-Forchheimer regime the flow becomes increasingly more chaotic in actual porous media and an inertial core region can develop. Figure 4demonstrates that the microrotation decreases with the increase in inertial parameter Fs, though the variation is not very prominent. The influence of chemical reacting parameter (χ) is depicted in Figure 6 and 7 for wide range of parametric values. The value of χ is taken as 0, 0.1, 0.3 and 0.5. This has been observed from the figure that for the higher value of χ the velocity is decreases. As χ increases the profiles become more monotonic in nature; in particular the gradient of the

profile becomes much steeper for $\chi = 0.5$than for lower values of the chemical reaction parameter. Figure 8 shows the variation of of the buoyancy ratio (N_b) and Chemical reaction parameter χon the dimensionless volume rate,Q. This is to be observed that an increment in the buoyancy ratio(N_b), from 0 to 5 that leads to excess of fluid velocity. Therefore, this can be written as the increasing the volume flow rate Q of the fluid through the channel. However, an increase in the Chemical reaction parameter χlead to a decrease in the volume flow rate through the channel. This would be consistent with the decrease in linear velocity. The expression of Q is shown in equation (18) which is obtained by integrating linear velocity across the channel width [$Q=\int_0^1 UdY$] indicating a direct proportionality between the volumetric flow rate and linear velocity field. Figure 9 is shown thevariation of the dimensionless total heat rate added to the fluid E with the buoyancy ratioN_b for distinguished values of vortex viscosity parameters as $R = 0,0.1,0.3, and\ 0.5$ respectively. This has been notices that an increase in buoyancy ratio will enhance the fluid flow and so the heat transfer between the two vertical plates. This also be came into the notice that average increases heat rate added to the fluid in the channel. The equation (19) viz , [$E=\int_0^1 U\theta dY$] , gives the linear relationship between E and U and θ.This also can be noted that as the vortex viscosity parameter increases, the total heat rate added to the fluid decreases, indicating that micropolar fluids can serve as coolants in engineering processes. Micro-structure clearly reduces heat transfer rates in the channel. Finally the dimensionless total species rate added to the fluid volumeφ is plotted as a function of the buoyancy ratio N_b for different values of Chemical reaction parameter χ, in Figure10. From equation (20), $\varphi = \int_0^1 U\Phi dY$, i.e. a direct linear relationship exists between φ and Φ. It is apparent that an increase in the buoyancy ratio increases the fluid flow which leads to an increase in the total species rate added to the fluid between the two vertical walls. Total species rate added to the fluid in the vertical channel also clearly decreases with an increase in Chemical reaction parameter χ, which as described earlier decreases the linear velocity field and therefore also φ.

5. CONCLUSIONS

The Chemically reacting free convective micropolar fluid flow between vertical parallel plates containing an isotropic, homogenous, Darcy-Forchemier porous medium has been studied. The Finite Element method is successfully implemented in non deimensional physical model.The numerical study shown the following:

I. The linear velocity (U) increases with the increase in Darcy Number (Da) .However it decreases with an increase in Forchheimer drag(Fs) and Chemical reaction parameter χ

II. This also observed that the angular velocity(H) increases with a rise in Darcy Number, Da,. However it decreases with an increase in Forchheimer number(Fs) and Chemical reaction parameter χ

III. The skin friction at the left plate, $U'(0)$ continuously decreases with the increase in Chemical reaction parameter χ .

IV. From the table this is observed that Nusselt number (Heat transfer rate) $-\theta'(0)$, increases with when there is an increment in thermal conductivity parameter, S. This parameter may be used as to control the rise in the temperature in industrial systems.

The results also shows that the (R > 0) possess a lower volumetric flow rate, total heat rate added to the fluid. Along with that the total species rate added to the fluid in comparison with Newtonian fluids (R = 0)

6. ACKNOWLEDGEMENTS

One of the Author V. Dabral is thankful to Department of Mathematics , HNB Garhwal Univefrsity, Srinagar for carried out the research work

REFERENCES

[1] Ingham D B & Pop I, *Transport Phenomena in Porous Media*, Vol II, Pergamon, Oxford (2002).
[2] Nield,D. A. Bejan,A. *Convection in Porous Media*, Second Edn, Springer, New York (1999).
[3] Rawat S & Kapoor S,"Procedia Engineering ", Elsevier, Vol 38, pp. 2288-2296, 2012
[4] Churchill S W& Chu H H S, *Int. J. Heat Mass Transfer,* 18, 1323- 1329 (1975).
[5] Nakayama A &Koyama H, *Heat Mass Transfer J.*, 28, 1041-1045 (1995).
[6] Rawat S, Bhargava R , Kapoor S, Bég O A, BégT A &Bansal R, ***J**ournal of **A**pplied **F**luid **M**echanics*, Vol. 7, No. 2, pp. 249-261, 2014
[7] Rawat S, Kapoor S & Bhargava R, *Journal of Applied Fluid Mechanics*, Vol 9, No 1, pp. 321-331 (2016)
[8] Rawat, S., Bhargava, R., Int. J. of Appl. Math and Mech., 5, 58-71, 2009.
[9] Bhargava R, Kumar L &Takhar H S, *Int. J. Engineering Science*, 41, 123-136 (2003).
[10] Beg, O.A., Zueco, J., Rawat, S. and Ghosh, S. K., Emirates Journal for Engineering Research, 14: 59-74, (2009)
[11] Rawat S, Bhargava S, Beg O A, Bhargava B R, Emirates Journal for Engineering Research, 14, pp. 77–90, (2009)

[12] Mohmoud M A A, *Physica A*, 375, 401-410, (2007)
[13] Cheng C Y, *Int. Communications in Heat Mass Transfer*, 33, 627-635 (2006).
[14] Gorla R S R., Takhar H S.&Slaouti, A,*Int. J. Engineering Science*, 36, 3, 315-327 (1998).
[15] Reddy, J.N., *An Introduction to the Finite Element Method*, MacGraw-Hill, New York (1985).
[16] Bathe, K.J., *Finite Element Procedures*, Prentice-Hall, New Jersey (1996).
[17] Dybbs A, & Edwards R.V, *NATO, ASI Series E, Applied Sciences*, *(Editors: Bear, J. and Corapcioglu, M.Y.)*, Vol. 82 (1984).
[18] Rees D A S & Pop I. *J. Applied Mathematics*, 61, 179-197 (1998).
[19] Rawat .S, & Kapoor S., Indian J. of Pure and Applied Physics, 55, 3269-3281 (2017)

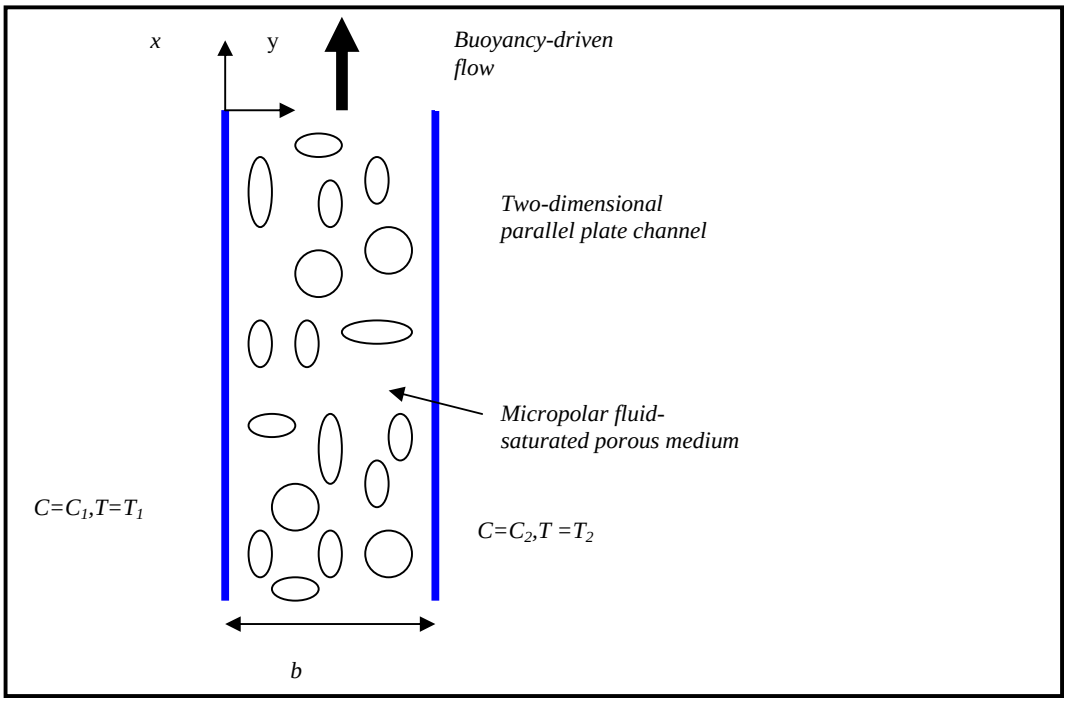

Figure1: Physical Model and Co-ordinate System

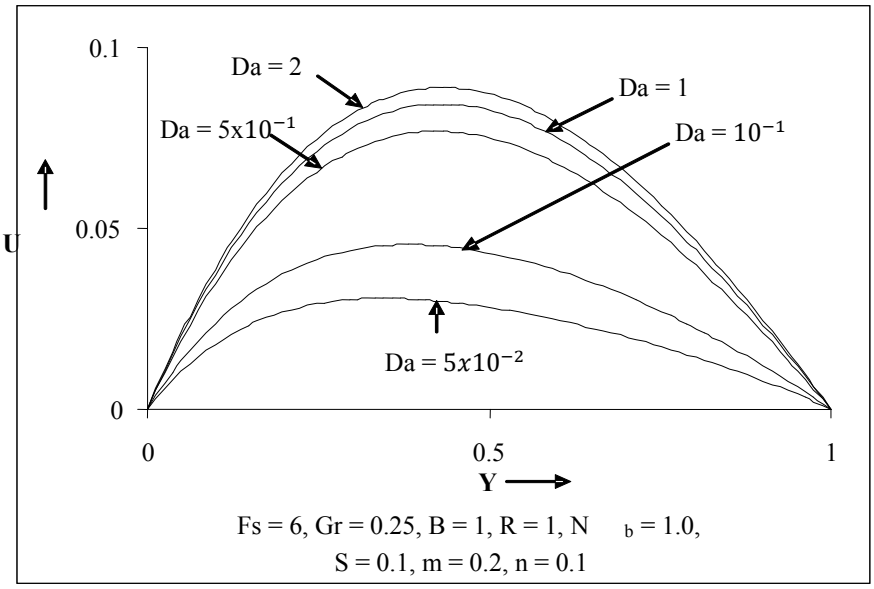

Figure2: Linear Velocity U versus Y for different values of Darcy number Da

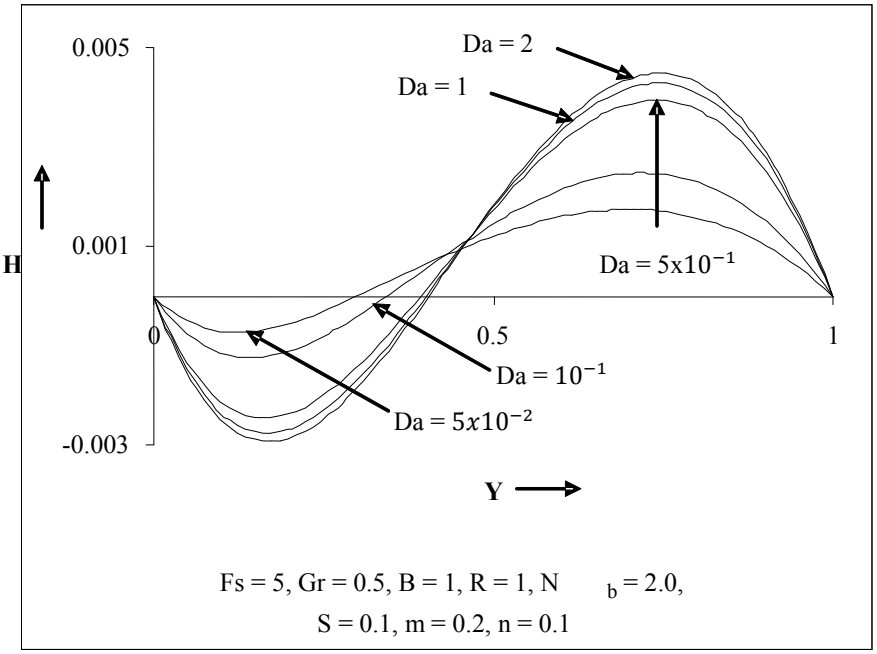

Figure 3: Angular velocity H versus Y for various values of Darcy number Da

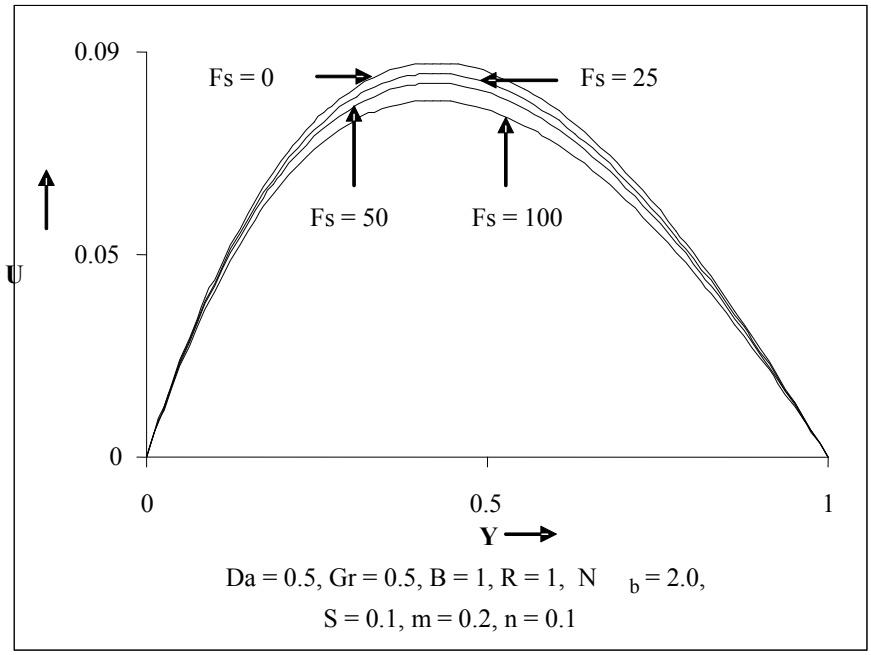

Figure 4: Linear Velocity U versus Y for different values of Forchheimer Drag Fs

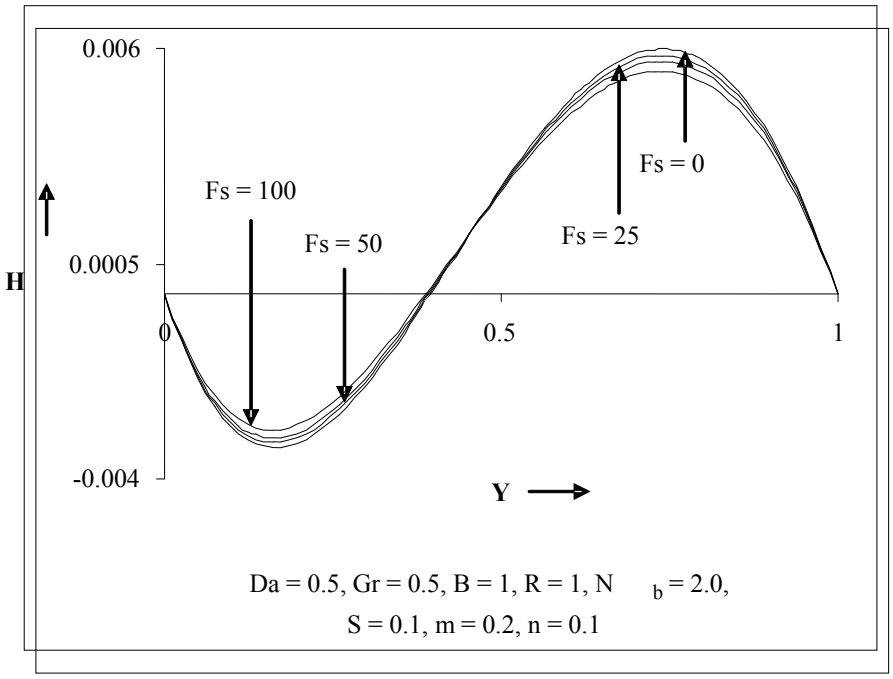

Figure 5: Angular velocity H versus Y for various Forchheimer Drag Fs

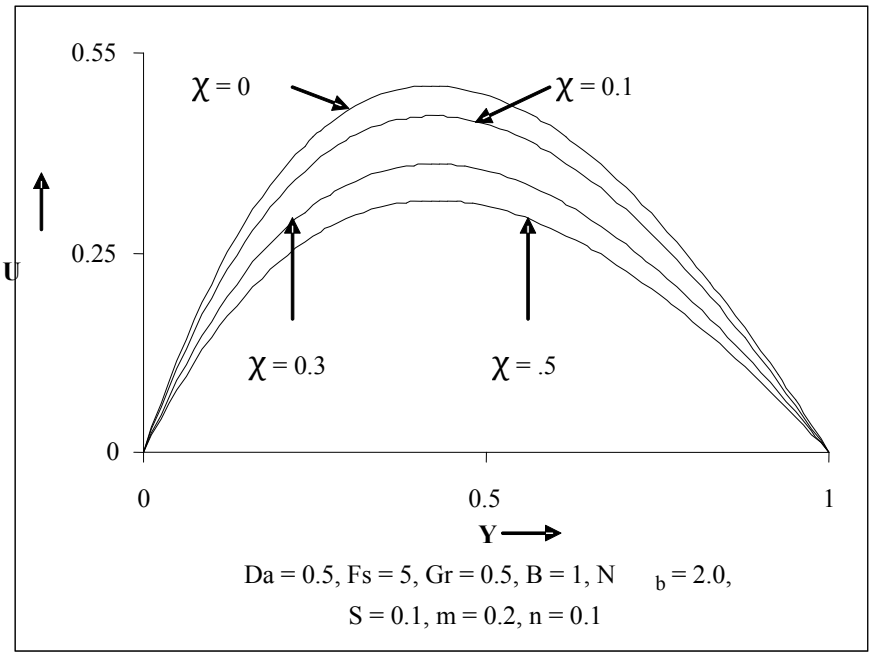

Figure 6: Linear Velocity U versus Y for various values of Chemical reaction parameter χ

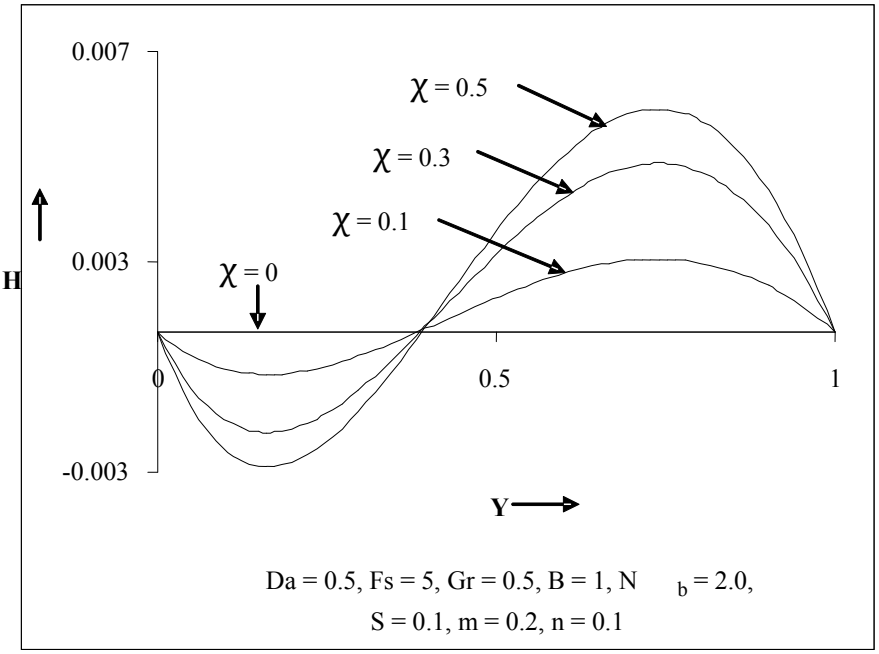

Figure 7: Angular velocity H versus Y for various values of Chemical reaction parameter χ

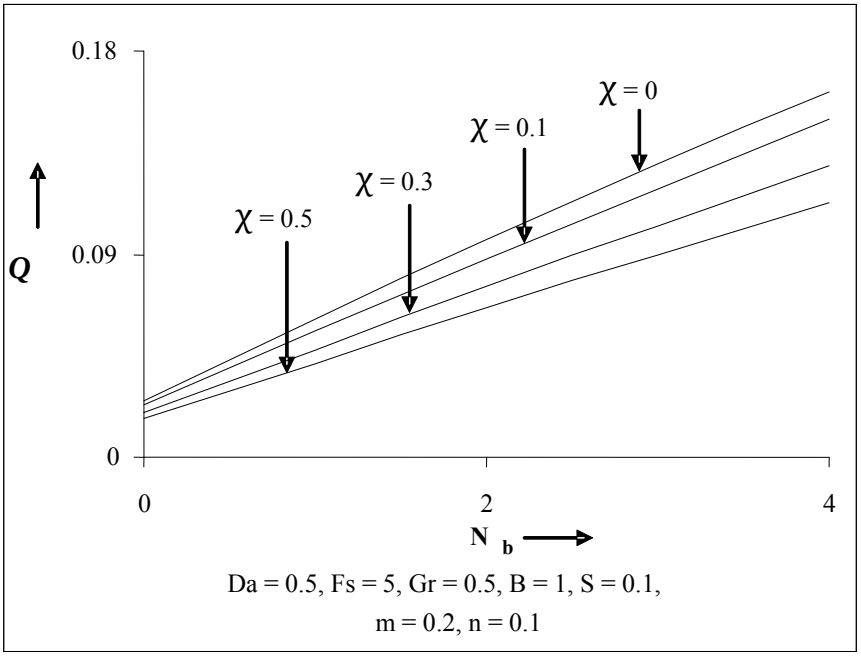

Figure 8: Dimensionless volume rate Q versus Buoyancy Ratio N_b for various Chemical reaction parameter χvalues

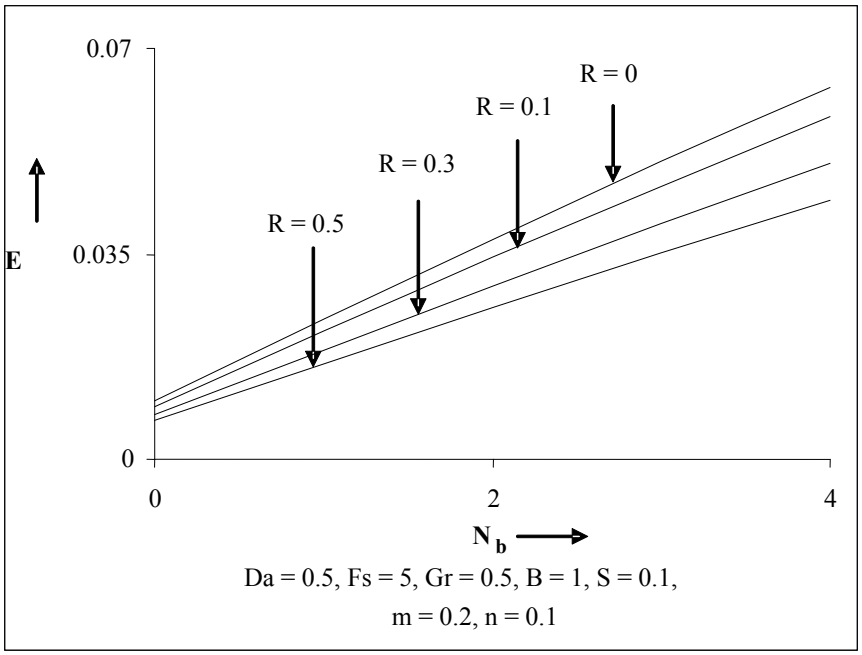

Figure 9: Dimensionless total heat rate added to the fluid E versus Buoyancy Ratio N_b for various vortex viscosity parameters as *R*

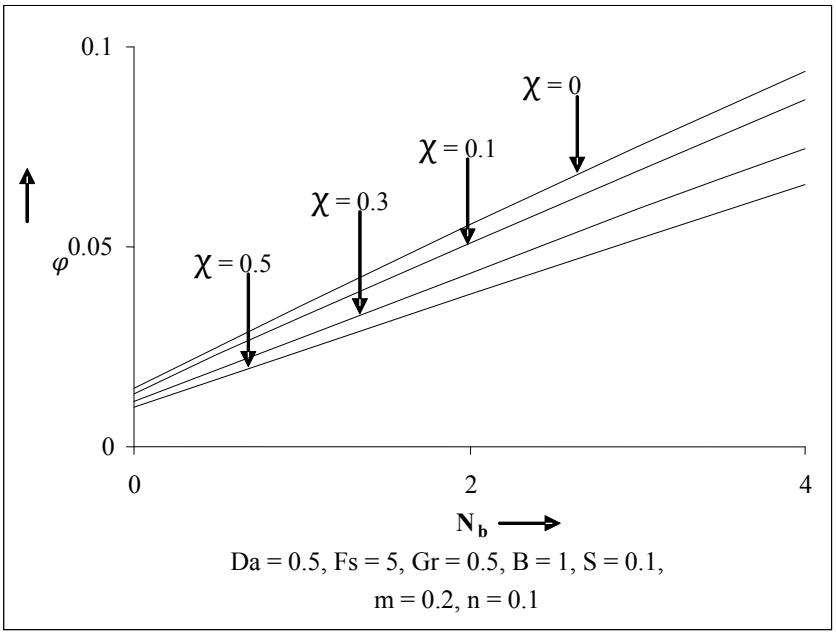

Figure 10: Dimensionless total species rate added to the fluid volumeφ versus Buoyancy Ratio N_b for various Chemical reaction parameter χvalues

Table 1: Values of $U'(0)$ and $-U'(0)$for different values of S

$Da = 10^{-1}, Fs = 10, Gr = 5x10^{-1}, B = 1, R = 2, \chi = 0.5, N_b = 2.0, m = 0.2, n = 0.1$		
S	$U'(0)$	$-\theta'(0)$ (Nusselt number)
0	0.493513	0.8
0.1	0.410347	3.74051
0.2	0.389244	6.73164
0.3	0.377834	9.41202
0.4	0.370811	11.7833
0.5	0.361011	12.0013

Table 2: Comparison Table of Finite Difference and Finite Element Computations

$Fs = 0.5, Gr = 0.5, B = 1, R = 1, \chi = 0.01, N_b = 2.0, S = 0.1, m = 0.2, n = 0.1$				
	$U\,(Da = 1.0)$		$H\,(Da = 1.0)$	
Y	FEM	FDM	FEM	FDM
0	0	0	0	0
0.090000	0.03721309	0.03724191	-0.00235331	-0.00235342
0.250000	0.06485041	0.06490212	-0.00262644	-0.00262681
0.450000	0.08444589	0.08444366	0.00055801	0.00055810
0.650000	0.06846551	0.06846319	0.00388112	0.00388923
0.8500000	0.02643509	0.02643745	0.00300619	0.00300112
1	0	0	0	0